

## Nuclear Scattering of 17-Mev Gamma-Rays

MARY BETH STEARNS\*

*Laboratory of Nuclear Studies, Cornell University, Ithaca, New York*

(Received April 17, 1952)

The nuclear scattering of gamma-rays from the  $\text{Li}^7(p, \gamma)\text{Be}^8$  reaction has been measured. The scatterers used were Bi, Pb, Sn, and Cu. The observed  $Z$  dependence of the elastically scattered gamma-rays varied as  $Z^{2.6 \pm 0.5}$ , while the inelastically scattered gamma-rays varied at a rate greater than  $Z^{2.9 \pm 0.3}$ . An appreciable amount of inelastic scattering was observed.

The elastic scattering results combined with previously measured integrated  $\gamma$ - $n$  cross sections of Cu are in agreement with a gamma-ray absorption curve centered around 17-18 Mev and having a width of 4-6 Mev.

### I. INTRODUCTION

FROM the study of the internal conversion of gamma-radiation of naturally radioactive nuclei it has long been recognized that the intensities of dipole and quadrupole transitions for these gamma-rays are about equally strong. This result was at first surprising since quadrupole transitions should be about a factor of  $(R/\lambda)^2$  weaker than dipole transitions. For even the heaviest nuclei and 1-Mev gamma-rays, this gives  $(R/\lambda)^2 \sim 1/250$ . Bethe<sup>1</sup> was able to explain this discrepancy by showing that the dipole transitions are greatly inhibited by correlations between the motions of the nucleons. Thus, these low energy gamma-rays do not have sufficient energy to disrupt the correlations between the nucleons and therefore the dipole transitions are seldom excited. However, in recent years, photoinduced reactions with gamma-rays of energies greater than 12 Mev have been observed and studied by many groups. In the energy region between 15 and 25 Mev, gamma-rays are absorbed strongly by all nuclei indicating that dipole transitions are involved. Here the gamma-rays seem to have enough energy to break up some of the correlations between the nucleons. From the investigations of these photoinduced processes it is therefore hoped to learn more about the type and behavior of the subunits in nuclei.

The photoinduced reactions consist of a nucleus first being excited by absorbing a photon and then decaying by the emission of one or more particles or gamma-rays. The reactions investigated up to the present time have been mainly those in which neutrons or protons are the particles emitted. A qualitative picture of the photoinduced reactions which agrees with the experimental results thus far is the following. The gamma-rays are absorbed in a dipole mode by a nucleon or small group of nucleons in the nucleus. This nucleon then usually interacts with the rest of the nucleons in the nucleus, producing a compound state. However, a small fraction of the time the excited nucleon escapes directly with no interactions, and therefore in these cases particles of high energies are emitted with dipole

angular distributions. With this picture, the energy distribution of the emitted particle agrees with the statistical model distribution at low energies but possesses a high energy tail whose angular distribution is symmetrical with a maximum at  $90^\circ$ , as shown in several experiments.<sup>2,3</sup>

As a first attempt to explain the observed results theoretically, Goldhaber and Teller<sup>4</sup> assumed that the gamma-rays excite the whole nucleus into a dipole mode of vibration. This dipole vibration was pictured as a motion in the nucleus in which the bulk of the protons moved in one direction and the bulk of the neutrons in the opposite direction. They further assumed that the coupling between the dipole vibration and other modes of nuclear motion was weak and that only the levels near the first excited level of the dipole vibration were important. These assumptions then yield a one-level theory in which the absorption of gamma-rays is effectively due to the first excited level of a simple harmonic dipole vibration of the entire nucleus; however, this level may be broadened by coupling with other nuclear motions. Since their theory contains only one energy level, they predict that most of the scattered gamma-rays should be elastic and that the integrated cross section for the scattering of gamma-rays should be an appreciable fraction of the total absorption cross section.

More recently, Levinger and Bethe<sup>5</sup> showed that one obtains the same total absorption cross section as Goldhaber and Teller by using only the assumption of dipole absorption of the gamma-rays, without any assumptions about the modes of vibration of the nucleus. That is, one gets the same total cross sections whether the nucleus as a whole or a single nucleon or some subunit of the nucleus absorbs the gamma-rays. They also considered the effects of exchange forces, intrinsic range, and type of well of the  $n$ - $p$  potential

<sup>2</sup> B. C. Diven and G. M. Almy, *Phys. Rev.* **80**, 407 (1950).

<sup>3</sup> P. R. Byerly, Jr., and W. E. Stephens, *Phys. Rev.* **83**, 54 (1951); Curtis, Hornbostel, Lee, and Salant, *Phys. Rev.* **77**, 290 (1950); H. L. Poss, *Phys. Rev.* **79**, 539 (1950); M. E. Toms and W. E. Stephens, *Phys. Rev.* **82**, 709 (1951); D. H. Wilkinson and J. H. Carver, *Phys. Rev.* **83**, 466 (1951).

<sup>4</sup> M. Goldhaber and E. Teller, *Phys. Rev.* **74**, 1046 (1948). See also H. Steinwedel and J. H. D. Jensen, *Z. Naturforsch.* **5a**, 414 (1950).

<sup>5</sup> J. S. Levinger and H. A. Bethe, *Phys. Rev.* **78**, 115 (1950).

\* Now at Nuclear Research Center, Carnegie Institute of Technology, Pittsburgh, Pennsylvania.

H. A. Bethe, *Revs. Modern Phys.* **9**, 71 (1937), Secs. 87 to 90.

on the total absorption cross section. Since the Levinger-Bethe theory allows many energy levels, it predicts that there will be some inelastic scattering of gamma-rays. This theory, therefore, also predicts that the cross section for the inelastic scattering of gamma-rays will be smaller than predicted by the Goldhaber-Teller theory.

Courant<sup>6</sup> proposed a direct photodisintegration process, which hypothesized that the gamma-ray is absorbed by a nucleon in the nucleus and the nucleon is then emitted directly without the formation of an intermediate compound nucleus. This model would explain the particles which are emitted with higher energies than would be expected from a statistical model. It also agrees with the high energy particles having angular distributions with a maximum at  $90^\circ$  as is observed experimentally. Small amounts of this direct interaction also make plausible the high ratios of  $(\gamma, p)$  to  $(\gamma, n)$  yields which were obtained for moderately heavy nuclei and which were much too high to be accounted for by a statistical model.

The purpose of this experiment is, therefore, to gain more information about these photoinduced nuclear reactions by studying the nuclear scattering of gamma-rays. From the magnitude and  $Z$  dependence of the scattering one can learn more about the "resonance" properties and nuclear model needed to explain gamma-ray absorption. If appreciable inelastic scattering is observed, it indicates that the simple one-level model of the Goldhaber-Teller theory cannot be correct without modification.

Previously two experiments have been performed to detect the nuclear scattering of gamma-rays. The first, by Gaerttner and Yeater,<sup>7</sup> was done by attempting to detect the scattered gamma-rays of a 100-Mev betatron by producing pairs in a cloud chamber. The cloud chamber was placed such that the gamma-rays had to be scattered through an angle of  $120^\circ$  within a spread of  $45^\circ$ . They state that if the assumption is made that all their observed pairs are from nuclear scattering then "the scattering in C and Cu is less than 1 percent and 3 percent, respectively, of the total cross section for resonance absorption," as predicted by the Goldhaber-Teller theory. However, they point out that all the observed pairs can probably be accounted for by bremsstrahlung from the secondary electrons in the scatterers.

The other measurement of scattered gamma-rays was made by Dressel, Goldhaber, and Hanson.<sup>8</sup> They placed Pr foils at  $90^\circ$  and  $145^\circ$  to the gamma-ray beam of a 22-Mev betatron. Then, using Pb as the scatterer, they measured the activity produced due to the  $\text{Pr}^{141}(\gamma, n)\text{Pr}^{140}$  reaction. Their final cross sections for Pb were:  $(d\sigma/d\omega)_{90^\circ} = 1.1 \pm 0.6$  mb/sterad;  $(d\sigma/d\omega)_{145^\circ} = 2.0 \pm 1.0$  mb/sterad.

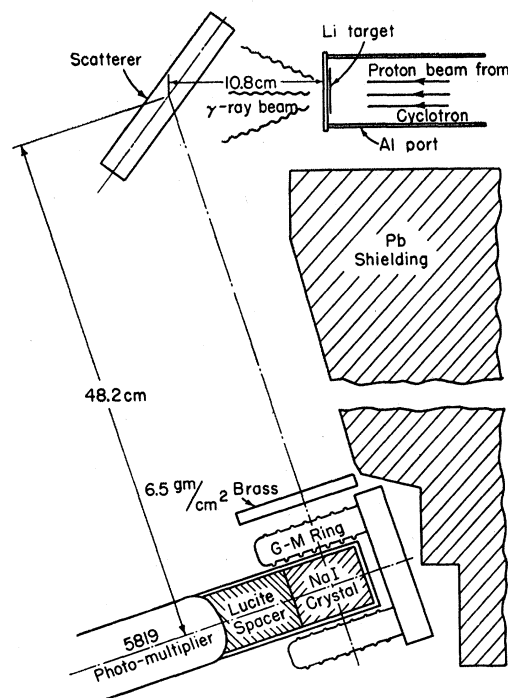


FIG. 1. Experimental arrangement of gamma-ray source, scatterer, and detector.

## II. APPARATUS

The experimental arrangement used to study the scattering of gamma-rays is shown in Fig. 1.

The gamma-rays to be scattered were produced by bombarding a thick Li target with 700-keV protons from the Cornell cyclotron. The scatterers used were Bi, Pb, Sn, and Cu. Each element was molded into a block from cp grade stock and then machined to be  $5 \times 5$  inches in area. The thicknesses were usually equal to the absorption mean free path of 17.6-Mev gamma-rays as measured by Walker.<sup>9</sup> Three Geiger counters were mounted above the source and used as monitors. Their counting rates throughout the experiment remained constant with respect to each other to within 2 percent.

The gamma-ray detector was a NaI(Tl) crystal which was in anticoincidence with a ring of Victoreen Geiger counters. The Geiger counters were staggered in position and thereby completely surrounded the crystal. They were all connected in parallel. The main function of the Geiger counters was to decrease the background due to cosmic rays. They reduced this background by factor of 8.5. The Geiger counters and anticoincidence arrangement also prevented detection of charged particles coming from the scatterer. However, this function was not very important since these particles were stopped by  $6.5 \text{ g/cm}^2$  of brass placed between the detector and scatterer as shown in Fig. 1.

<sup>6</sup> E. D. Courant, Phys. Rev. **82**, 703 (1951).

<sup>7</sup> E. R. Gaerttner and M. L. Yeater, Phys. Rev. **76**, 363 (1949).

<sup>8</sup> Dressel, Goldhaber, and Hanson, Phys. Rev. **77**, 754 (1950).

<sup>9</sup> R. L. Walker, Phys. Rev. **76**, 527 (1949).

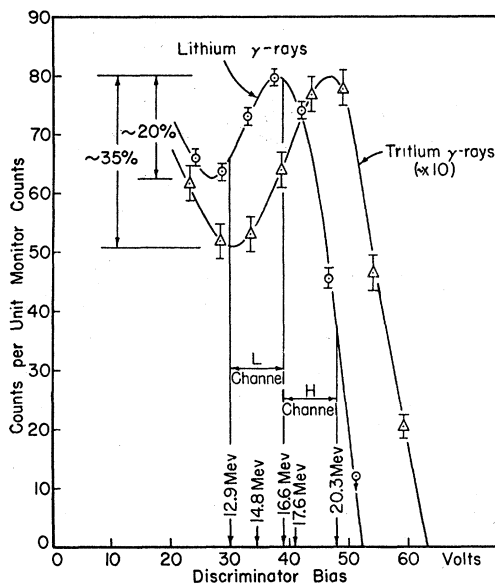


FIG. 2. Pulse-height distribution curves for Li and tritium gamma-rays. The pulse-height distribution curves were obtained by placing the NaI crystal directly in the beam and taking differential number—bias curves. The energy scale has been determined by assigning an energy of 17.6 Mev to the peak of the pulse-height distribution curve which would be obtained with monoenergetic gamma-rays of 17.6 Mev. The two indicated channels were those used for detection of the scattered gamma-rays.

The detector was shielded from the gamma-ray source as shown in Fig. 1.

The NaI(Tl) crystal was a cylinder 4 cm in diameter and 5 cm in height. Since the crystal was so large, it had a rather high efficiency (about  $\frac{1}{3}$ ) for detecting gamma-rays in the energy region of around 16 Mev. By measuring the height of the pulses coming from the crystal, one could also obtain energy discrimination of the gamma-rays. The crystal was mounted by immersing it and a 5-cm Lucite spacer into mineral oil in a hollow Lucite cylinder. The hollow cylinder had all its inner surfaces lined with reflectors, a mirror cemented to the end opposite the phototube, and an Al foil along the inside wall. This assembly was then optically connected to the phototube window by a thick coating of Canada balsam.

The main factors that made this experiment more sensitive than previous experiments were the increase in efficiency of detection of the gamma-rays by the use of the NaI(Tl) crystal and the decrease in background obtained by having the Geiger counters in anticoincidence with the crystal.

The over-all electronic system, from the input at the phototube and through to the pulse-height discriminator and recording scalars, was checked for linearity many times throughout the experiment and was never found to deviate from linearity by more than 2 percent.

The discriminators were units of a multichannel discriminator, and the voltage intervals between them were fixed by batteries. The zero of the discriminator

system was checked frequently while running and was never found to vary by more than 2 percent of the channel width. The channel widths were 9 volts.

The cosmic-ray background was measured about every other day while running and was constant within the statistics. The lithium pulse-height distribution was also taken throughout the experiment and remained the same over periods of days. The recording apparatus was always left on over night, with the counter high voltage off. This allowed one to determine if any pulses from the power line or elsewhere were being picked up.

The detection system was also checked to determine whether the anticoincidence circuit was causing any unusual behavior. This was done by counting with the crystal in the direct beam and with and without the Geiger counters on. Within the accuracy of the apparatus, the results under both conditions were the same.

### III. AUXILIARY MEASUREMENTS

#### Characteristics of the Detector

The lithium gamma-ray pulse-height distribution was obtained by placing the NaI(Tl) crystal directly in the beam and taking differential number—bias curves. The result of these measurements is shown in Fig. 2. One sees that the crystal detector does not resolve the 14.8-Mev and 17.6-Mev lines of the lithium spectrum. The resolution of the crystal is poor because a large fraction of the time the pairs formed by the gamma-rays do not lose their full energy in the crystal. Two things can happen to cause this. Either the members of the pairs may not be completely stopped in the crystal but leave it before losing all their energy, or else they may emit bremsstrahlung and the created gamma-rays leave the crystal without interacting. One can qualitatively understand the observed distribution curve in Fig. 2, as a compound distribution of the 14.8-Mev and 17.6-Mev lines, if the response of the detector to monoenergetic gamma-rays is known. For this purpose a measurement was made of the pulse-height distribution of the 20-Mev monoenergetic gamma-rays obtained by bombarding tritium with 0.96-Mev protons. This is also shown in Fig. 2. To obtain the expected pulse-height distribution for the 14.8-Mev and 17.6-Mev lines from this measurement at 20 Mev, one has to assume that the shape of the distribution curve for monoenergetic gamma-rays does not vary with energy over the energy region from about 14 Mev to 20 Mev. This assumption is reasonable in view of the following facts. The resolution of the detector for ThC'' gamma-rays (2.62 Mev) was measured and found to be about 15 percent, while near 17 Mev it is 28 percent. Therefore, while the resolution of the detector does vary some with energy, it does not do so very rapidly. Thus, between 14–20 Mev it should be a reasonable assumption to suppose that it stays constant. If the separate lithium lines are therefore given shapes corresponding to that obtained from

the tritium pulse-height distributions and are then added together in the proper ratios, they reproduce very well the observed lithium pulse-height distribution shown in Fig. 2.

Energy sensitivity curves for the various channels can also be obtained using the monoenergetic gamma-ray pulse-height distribution. They are shown in Fig. 3. Again one has to assume that the shape of the distribution curve remains constant over the range of about 13–20 Mev. The energy sensitivity curve for a given discriminator setting is obtained by reflecting about its peak, the monoenergetic gamma-ray pulse-height distribution for that energy gamma-ray that has the peak of its distribution curve at the energy that corresponds to the discriminator setting. Therefore, to get the energy sensitivity of a channel with a finite width one must add up the sensitivity curves for all points in the energy range of the channel. The energy sensitivity curves, for each of the single channels used in the experiment, were obtained by adding the sensitivity curves for three equally spaced points in the channels. The energy sensitivity curve for both channels taken together was then obtained from the sensitivity curves of the two single channels. From these curves it is possible to obtain the effective range of gamma-ray energies for which each channel is sensitive.

Two separate runs of the whole experiment were made. In the first run the detector had a resolution of 33 percent, and only one energy channel was used. The energy biases for this channel were 12.9 Mev and 21.8 Mev, based on an energy scale which would correspond to assigning the energy of 17.6 Mev to the peak of the pulse-height distribution curve that would be obtained from a monoenergetic gamma-ray of 17.6 Mev. For this channel 90 percent of the area under the sensitivity curve below 17.6 Mev was due to gamma-rays of energies greater than 12.0 Mev. In the second run the detector had been remounted, and it now had a resolution of 28 percent; also two energy channels were used. The energy biases were 12.9 Mev and 16.6 Mev for the low energy channel (called the *L* channel) and 16.6 Mev and 20.3 Mev for the high energy channel (called the *H* channel). For the *H* channel 90 percent of the area under the sensitivity curve below 17.6 Mev was due to gamma-rays of energies greater than 14.4 Mev, while in the two channels taken together (called the *HL* channel) 90 percent of the area of sensitivity below 17.6 Mev was due to gamma-rays of energies greater than 12.3 Mev.

The average energies detected by the various channels depends on the spectrum of the gamma-rays incident on the crystal. If the energy spectrum of the incident gamma-rays is represented by a function  $f(E)$  and the energy sensitivity of the channel is given by a function  $S(E)$ , then the average energy is given by

$$\bar{E} = \frac{\int_0^{17.6 \text{ Mev}} E f(E) S(E) dE}{\int_0^{17.6 \text{ Mev}} f(E) S(E) dE}. \quad (1)$$

Since the spectra of the scattered gamma-rays are not known, the average energy of detection of the channels is in general not known. However, the spectrum is known when looking at the direct beam, and, therefore, the average energy for the various channels can be obtained for this condition. The average energies of detection for the direct beam, obtained in this manner, are 16.9 Mev for the *H* channel and 16.3 Mev for the *L* channel.

### Identification of Particles

The experiment was run with 6.5 g/cm<sup>2</sup> of brass between the scatterer and detector. This caused electrons of 15 Mev to lose about 11 Mev in the brass. In this way electrons were prevented from producing pulses large enough to be recorded by the energy channels. Any other charged particles would also lose at least this much energy in the brass, and they also could not be recorded by the detection system. It can therefore be concluded that the counts from the scatterer were not due to charged particles.

It is true that there might be a small amount of conversion of some of the energy of the secondary electrons into gamma-rays in the brass. However, the number of gamma-rays that might be formed in this way is entirely negligible compared to the number that might be formed in the scatterer itself. Therefore, there is little advantage to be obtained by using a lower *Z* element, like Al, in

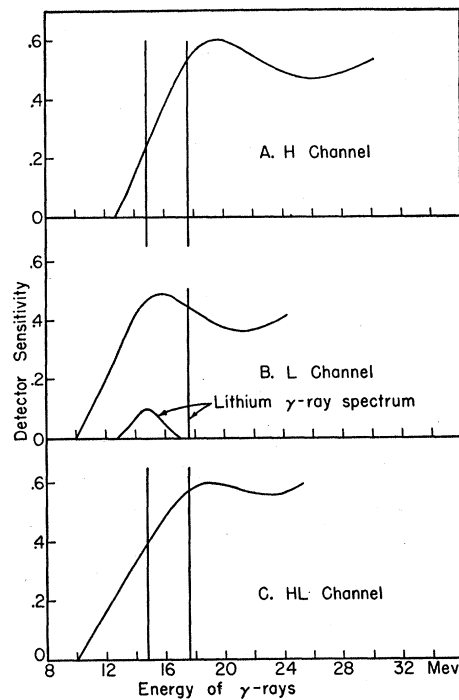


FIG. 3. Energy sensitivity curves for the various energy channels. In obtaining these curves the assumption is made that the shape of the pulse-height distribution curves for monoenergetic gamma-rays remains constant over the energy region from 13–20 Mev.

place of the brass. The brass has the advantage that it is much more compact. This bremsstrahlung production by the secondary electrons is considered later in more detail.

It would be extremely improbable for the gamma-rays to give rise to the emission of neutrons of sufficiently high energy to be detected by the crystal. At best the neutrons could be emitted with about 17 Mev minus their binding energy. Also the efficiency of the NaI(Tl) crystal for detecting neutrons is extremely small. But, to make certain that neutrons were not being detected, a run was made with a block of paraffin between the scatterer and detector. A thickness of paraffin of one mean-free-path for 12-Mev neutrons was used. If the counts were due to neutrons, the counting rate with the paraffin should have been reduced to 37 percent of the counting rate without the paraffin. However, if the counts were due to gamma-rays, the paraffin should have reduced the counting rate to 80 percent of that without the paraffin. Normalizing the counting rate without the paraffin to be  $1.0 \pm 0.15$ , the results were that with the paraffin in place the counting rate was  $0.75 \pm 0.12$ . This then indicates that the counts were due to gamma-rays and not neutrons.

To check further that the counts from the scatterer were due to gamma-rays, runs were made with a Pb absorber, of two mean-free-paths for 17-Mev gamma-rays, inserted between the scatterer and detector. If the counts were due to gamma-rays, this amount of Pb

should have a transmission of 0.13. Taking the normalized counting rate without the Pb absorber equal to  $1.0 \pm 0.09$ , the counting rate with the Pb absorber was  $0.11 \pm 0.09$ . This agrees well with the expected transmission, making it quite certain that what were being detected by the crystal were scattered gamma-rays.

#### IV. GENERAL PROCEDURE

The scattering of gamma-rays was measured for four different nuclei: Bi, Pb, Sn, and Cu. From these measurements the variation of the differential cross section with  $Z$  was obtained. The scattering measurements were made by alternately taking runs with the scatterers in place and without them. The number of scattered gamma-rays was then obtained for each run by subtracting the backgrounds adjacent to each scatterer run. In this way the total scattering measurement for each type of nucleus was made up of several individual runs. These individual runs were then used to compute an rms error, i.e., the error determined by taking the deviation from the mean of the separate runs. The statistical standard deviation for the total scattering measurements was also computed. In all cases the rms error agreed very well with the statistical error. This gave a good check on the stability and internal consistency of the data. All errors quoted in the results are the larger of the rms error or the standard deviation.

To be sure that the scattering observed was not due to gamma-rays from bremsstrahlung caused by the secondary electrons in the scatterer, the scattered gamma-rays were measured at three angles for Pb and Sn.

By counting with the detector in the direct beam and with the same energy channels as when measuring scattered gamma-rays, measurements were obtained which, when combined with the scattered gamma-ray measurements, allowed the absolute differential cross section for the nuclear scattering of gamma-rays to be determined.

The magnitude of the proton beam throughout the experiment was about 90–100  $\mu$ a when measuring scattered gamma-rays and about 20–25  $\mu$ a when making measurements of the direct beam. A beam of 90–100  $\mu$ a of 700-keV protons striking a thick lithium target yields about  $10^7$  gammas/sec. In the *HL* channel the counting rates for gamma-rays scattered through  $116^\circ$  were about as follows: Bi, 1.4 counts/min; Pb, 1.2 counts/min; Sn, 0.75 count/min; Cu, 0.35 count/min; cosmic-ray background, 0.8 count/min; and background with no scatterer, 1.6 counts/min. These are the counting rates for each scattering block. The scatters did not contain equal number of nuclei. The counting time per observation was about 35 minutes. At  $116^\circ$  a total scattering measurement was comprised of about eleven separate runs consisting of counting both with and without the scatterer in the beam.

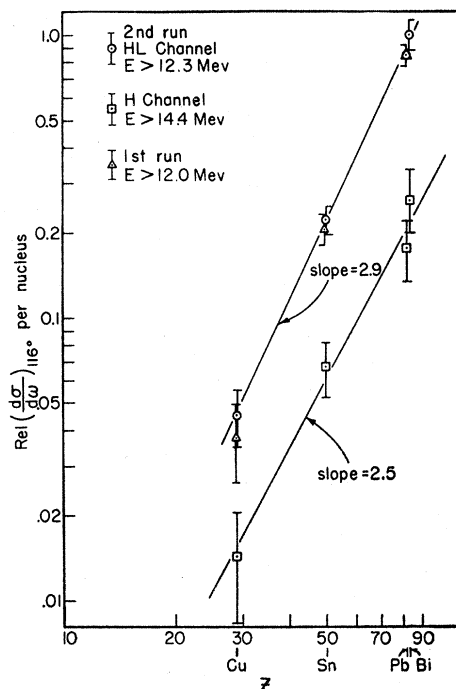


FIG. 4. Variation of the relative differential nuclear scattering cross section per nucleus as a function of  $Z$ . The average angle of scattering was  $116^\circ \pm 17^\circ$ .

## V. RESULTS

## Z Dependence

Figure 4 shows the  $Z$  dependence of the differential cross section per nucleus at an average angle of scattering of  $116^\circ \pm 17^\circ$ . The average angle of scattering is determined from the measured angle ( $108^\circ$ ) by the application of three geometric weighting factors. The first factor weights the angles of scattering from different portions of the scatterer by the solid angle subtended at the source. This is a large correction since some portions of the scatter subtend about four times the solid angle that others subtend. The second correction comes about because the detector subtends different solid angles for different portions of the scatterer. The largest variation in detector solid angle for the various portions is only 25 percent; therefore, this correction is much smaller than the first correction. It is also in the opposite direction. The third correction is due to the variation in distance that the gamma-rays travel before and after being scattered in the different regions of the scatterer. This correction is also much smaller than the first correction and in the opposite direction. The greatest variation between various portions of the scatterer is about 25 percent.

For the second run the counting rates for the various elements have been taken relative to Bi which has been normalized to 1. For the first run Bi was not measured, and the counting rates have been taken relative to Pb which has been normalized to the same value it had in run 2. It is seen that the agreement between runs 1 and 2 is excellent. Run 2 was made with much more care and accuracy than run 1, and only it will be considered from now on. Both the counting rate for the  $H$  channel and the  $HL$  channel have been plotted. Since the  $H$  channel does not detect many gamma-rays below 14.5 Mev, the counts in this channel are essentially due to elastic scattering. The differential cross-section variation determined from only the  $H$  channel data goes as  $Z^{2.5 \pm 0.5}$ . The differential cross-section variation from the  $HL$  channel data goes as  $Z^{2.9 \pm 0.3}$ .

While one might expect such a rapid variation with  $Z$ , as  $Z^{2.5}$ , for elastic scattering (due to a  $Z^2$  from coherence), it is at first surprising that the inelastic scattering should vary as strongly as  $Z^{2.9}$  or greater. Thus, it might be suspected that some process other than nuclear scattering is contributing to the  $HL$  channel data. The bremsstrahlung process mentioned before would be expected to go as about  $Z^4$  per nucleus ( $Z^2$  for pair production,  $Z^2/A$  for Coulomb scattering and  $Z^2/A$  for the bremsstrahlung emission). Therefore, one suspects that the strong  $Z$  dependence of the both channel data may be due to the bremsstrahlung process. So angular distribution measurements were made to investigate the bremsstrahlung more thoroughly.

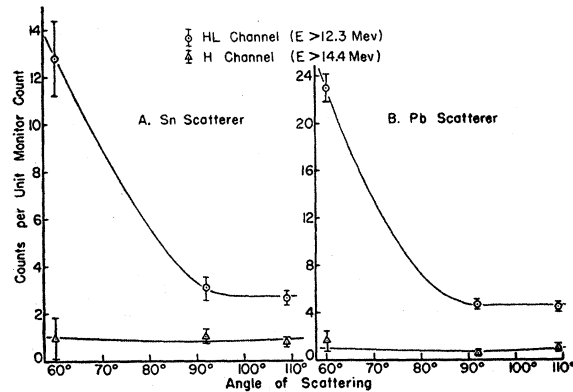


Fig. 5. Variation of the intensity of scattered gamma-rays from Pb and Sn as a function of the scattering angle. The data are plotted at the average bremsstrahlung angle of scattering. The line drawn through the  $H$  channel data corresponds to a  $(1 + \cos^2 \theta)$  distribution.

## Investigation of Possible Bremsstrahlung Contamination

The bremsstrahlung process comes about from the electrons and positrons, formed from pair production, being scattered through large angles and then emitting bremsstrahlung. To obtain information about the amount of bremsstrahlung present, measurements of the scattering were made at three angles for Pb and Sn. The three measured angles were  $108^\circ$ ,  $90^\circ$ , and  $62\frac{1}{2}^\circ$ . The average angles of scattering are determined by applying the previously mentioned three correction factors and also another correction factor depending on the type of scattering which the electron or positron undergoes. Rough information about the type of scattering can be obtained by using the curves of Snyder and Scott.<sup>10</sup> By considering these curves we conclude the following. At the two larger angles measured ( $90^\circ$  and  $108^\circ$ ), Coulomb scattering is the most important type of scattering. For the  $62\frac{1}{2}^\circ$  angle of scattering the multiple (or plural) scattering is about three times the single Coulomb scattering for the Pb scatterer and about two times the single scattering for the Sn scatterer. Therefore, for the two larger angles,  $90^\circ$  and  $108^\circ$ , we apply a Coulomb scattering angular dependence factor to obtain the average bremsstrahlung angle of scattering, while for the  $62\frac{1}{2}^\circ$  angle of scattering we know only that the angular dependence varies more rapidly than the Coulomb scattering angular distribution. When the formerly described three geometric correction factors and the Coulomb weighting factor,  $1/\sin^4(\theta/2) [1 + \beta^2 \sin^2(\theta/2)]$ , are applied to the two larger angles, the  $90^\circ$  scattering angle becomes  $92^\circ$  and the  $108^\circ$  angle becomes  $109^\circ$ . For the smallest angle ( $62\frac{1}{2}^\circ$ ) we shall estimate the average angle of scattering to be around  $60^\circ$ .

In Fig. 5 the variation of the number of scattered gamma-rays with the average scattering angle is shown.

<sup>10</sup> H. S. Snyder and W. T. Scott, Phys. Rev. **76**, 220 (1949).

These yields have been corrected for the different solid angles subtended by different regions of the scatterer, etc. (the first three geometric corrections mentioned above).

It can be seen that for both Sn and Pb the number of counts in the  $H$  channel stays essentially the same at all three angles. This indicates that little bremsstrahlung is being counted by the high energy channel. This is to be expected, since this channel measures essentially elastically scattered gamma-rays and any gamma-rays formed by the bremsstrahlung process would be degraded in energy. (The elastically scattered gamma-rays should have an angular distribution like  $(1+\cos^2\theta)$ . This variation, however, is within the statistics of the plotted points.)

The yield of scattered gamma-rays from the  $HL$  channel data rises rapidly as we go to smaller angles. (Since the inelastically scattered gamma-rays probably

TABLE I. Experimental values of quantities in Eq. (4).

Quantity	Bi	Pb	Sn	Cu	Units
$n_H$	$13.3 \pm 3.4$	$8.9 \pm 2.2$	$7.9 \pm 2.0$	$4.1 \pm 1.8$	$\frac{\text{counts}}{\text{monitor count}}$
$n_{HL}$	$49.6 \pm 6.2$	$42.7 \pm 3.8$	$26.5 \pm 3.1$	$12.9 \pm 3.0$	$\frac{\text{counts}}{\text{monitor count}}$
$N$	$2.82 \times 10^{22}$	$3.29 \times 10^{22}$	$3.79 \times 10^{22}$	$8.45 \times 10^{22}$	atoms/cm <sup>3</sup>
$\lambda$	1.07	1.49	3.04	3.26	cm
$t=0.80$ for 17-Mev gamma-rays.					
$C_{HL} = (2.00 \pm 0.04) \times 10^6$ counts/monitor count.					
$C_H = (0.96 \pm 0.02) \times 10^6$ counts/monitor count.					
$f\Omega_1 = 0.482$ steradians (a standard deviation of 10 percent is estimated for this quantity).					
$I_0/I_{90^\circ} = 1.09$ . <sup>a</sup>					

<sup>a</sup> The 440-kev resonance has a width of about 12 kev, and the nonresonant tail from 440 kev to 700 kev has an intensity of 2 percent of the peak of the 440-kev resonance [see W. A. Fowler and C. C. Lauritsen, Phys. Rev. **76**, 314 (1949)]. Therefore, at 0° a 700-kev proton beam incident on a thick Li target produces radiation which is about 30 percent nonresonant and 70 percent resonant radiation. Since the nonresonant radiation is anisotropic the 0° and 90°, intensities are therefore unequal (see reference 11).

are emitted from a compound state of the nucleus, it is assumed that they are isotropic. Therefore, if all the  $HL$  channel data were the result of nuclear scattering, it would remain constant at all angles.) This rapid rise shows that, at least at small angles, there is a large amount of bremsstrahlung emitted from the scatterers. Assuming that the observed counts are due only to nuclear scattering and bremsstrahlung, we can calculate the amount of bremsstrahlung present for the largest angle of scattering. The results obtained from the 90° data show that the bremsstrahlung process contributes about  $13 \pm 13$  percent in the 116° nuclear scattering measurement. In addition, the calculations from the 60° data indicate that the bremsstrahlung process contributes less than about 10 percent in the 116° scattering measurement.

An estimate of the amount of bremsstrahlung in the 116° scattering data can also be obtained by calcu-

lating the absolute differential cross section of the bremsstrahlung process. Starting with a 17.6-Mev gamma-ray striking a Pb scatterer and considering energy losses due to ionization, a detailed calculation was made of the probability of obtaining an electron or positron of a given energy which had been singly Coulomb scattered through a given angle. Next the probability of the electron emitting a gamma-ray of energy sufficient to be recorded by the  $HL$  channel was calculated. An integration was then made over all possible energies of the electron or positron. The absolute differential cross section obtained in this way was  $(d\sigma/d\omega)_{116^\circ} \approx 0.02$  mb/sterad.

As will be seen later, a lower limit for the observed differential cross section for scattering from Pb is  $1.2 \pm 0.2$  mg/sterad. Hence, it is seen that the estimate of the cross section for the single scattering bremsstrahlung process is only 2 percent of the observed lower limit of the cross section for the scattering of gamma-rays. Calculations considering two ( $54\frac{1}{2}^\circ$ ) scatterings instead of a single scattering yield differential cross sections about twenty times smaller than that of the above calculation. Nevertheless, there may exist combinations of plural and multiple scatterings that have probabilities that are as large or larger than the single scattering probability. However, these processes are rare, and it is therefore probably safe to assume that the single scattering process gives a reasonable estimate of the scattering process.

Since the above calculation of the cross section for the bremsstrahlung process is probably on the high side or in any case it yields a result that is much smaller than the measured cross section, the amount of bremsstrahlung in the data for the  $HL$  channel will be assumed to be small and be neglected in the analysis. The bremsstrahlung in the high energy channel will be assumed to be zero.

### Differential Cross Section of Nuclear Scattering

The absolute differential cross section for the nuclear scattering of gamma-rays can be determined by combining the scattering measurements with measurements of the direct beam. The direct beam measurements were obtained by simply placing the crystal at a known distance from the source in the direct beam and observing the number of counts per unit monitor count.

To assure that the phototube experienced the same fringe magnetic field from the cyclotron throughout all measurements, the crystal was kept at essentially the same location for detecting both scattered or direct gamma-rays. Therefore, for the direct beam measurements it was at about 90° to the incident proton beam. The crystal was also placed the same distance from the source for the direct beam measurements of scattered radiation. This assured that the detector subtended the same solid angle in both cases.

For the measurements with the crystal in the direct beam, the observed number of counts per unit monitor



count is given by

$$C = I_{90^\circ} \epsilon A_2 / d^2, \quad (2)$$

where  $C$  is the number of counts per unit monitor count with the crystal in the direct beam,  $I_{90^\circ}$  is the number of gamma-rays emitted from the source per unit monitor count per unit solid angle at  $90^\circ$  to the proton beam,  $\epsilon$  is the efficiency of the crystal for detecting gamma-rays,  $A_2$  is the effective area of the crystal, and  $d$  is the distance from the center of the detector to the center of the source or also from the center of the scatterer to the center of the detector ( $=48.2$  cm).

From the measurements of the scattered radiation, the observed number of counts per unit monitor count is given by

$$n = I_0 f \Omega_1 N (d\sigma/d\omega)_{116^\circ} \lambda (\epsilon A_2 / d^2) t, \quad (3)$$

where  $n$  is the number of scattered gamma-rays counted by the detector per unit monitor count,  $N$  is the number of atoms per  $\text{cm}^3$  in the scatterer,  $(d\sigma/d\omega)_{116^\circ}$  is the differential scattering cross section for an average angle of  $116^\circ$ ,  $\lambda$  is the mean-free-path for 17.6-Mev gamma-ray<sup>9</sup> (equal to the scatterer thickness),  $t$  is the transmission factor for 17-Mev gamma-rays going through the  $6.5 \text{ g/cm}^2$  of brass between the scatterer and detector,  $\Omega_1$  is the solid angle subtended by the scatterer at the source, and  $f$  is the absorption correction factor for the scatterers due to the variation in distance which the gamma-rays travel before and after being scattered in different regions of the scatterer. By substituting (2) in (3), we obtain

$$(d\sigma/d\omega)_{116^\circ} = [n / (N \lambda t C f \Omega_1)] (I_0 / I_{90^\circ}). \quad (4)$$

The values of the quantities to be used in Eq. (4) are given in Table I. Substituting the values for the various quantities into Eq. (4) yields the differential cross sections for the nuclear scattering of gamma-rays which are tabulated in Table II.

The efficiency used in these calculations is the efficiency for the detection of rather high energy gamma-rays, since it is obtained from the direct beam measurement. Owing to the fact that the energy sensitivity curves fall off very rapidly with decreasing energies (see Fig. 3), this efficiency is greater than the actual efficiency for detecting inelastically scattered gamma-rays. Therefore, the cross sections obtained from the *HL* channel data give only a lower limit for the scattering of the gamma-rays detected in this channel. As one can see from Fig. 3, the efficiency used probably does not differ from the actual efficiency by more than a factor of three. Therefore, the upper limits for the cross sections determined from the *HL* channel data are about three times the values listed in the above table.

The efficiency obtained from the direct beam measurement is, however, very nearly equal to the efficiency with which the elastically scattered gamma-rays are detected. Therefore, the cross sections obtained from

TABLE II. Differential cross sections for the nuclear scattering of the gamma-rays from the  $\text{Li}^7(p, \gamma)\text{Be}^8$  reaction. For the *H* channel 90 percent of the scattered gamma-rays have energies greater than 14.4 Mev. For the *HL* channel 90 percent of the gamma-rays have energies greater than 12.3 Mev.

Scatterer	$(d\sigma/d\omega)_{116^\circ}$ in mb/sterad		Estimates of accuracy of <i>HL</i> channel values
	<i>H</i> channel	<i>HI</i> channel	
Bi	$0.82 \pm 0.22$	1.5	$+3.0$ $-0.2$
Pb	$0.53 \pm 0.14$	1.2	$+2.4$ $-0.2$
Sn	$0.20 \pm 0.049$	0.33	$+0.66$ $-0.05$
Cu	$0.044 \pm 0.020$	0.07	$+0.13$ $-0.02$

the *H* channel data are correct. The errors given for these cross sections are standard deviations.

### Inelastic Scattering

With the crystal in the direct beam, the ratio of counts in the high channel to those in the low channel was  $0.93 \pm 0.03$ . The ratios observed for the scattered gamma-rays are given in Table III.

If the scattering were all elastic we should expect the ratio of counts in the high to low channels to be larger than 0.93 for the following three reasons: (1) The cross section for scattering probably has a maximum around 18–20 Mev and decreases at lower energies. Thus, the scattering of the higher energy gamma-rays is favored. (2) We know that the energy sensitivity curves fall off very rapidly at lower energies. Therefore, in the detection of the gamma-rays the higher energy gamma-rays are much favored over the lower energy gamma-rays. (3) The gamma-rays produced by 700-kev protons striking a thick lithium target have for the ratios of 17.6-Mev to 14.8-Mev gamma-rays values of 1.3 and 1.1, respectively, at  $0^\circ$  and  $90^\circ$  to the incident proton beam.<sup>11</sup> Therefore, the gamma-rays to be scattered have a slightly higher average energy than the directly measured gamma-rays. All three of these factors would then contribute to give more counts in the high channel than in the low channel. Therefore, to account for the large decrease in the high to low ratio of counts for the

TABLE III. Ratios of the number of counts in the *H* channel to those in the *HL* channel from the scattered gamma-rays.

	Scatterer			
	Bi	Pb	Sn	Cu
<i>H</i> channel counts				
<i>HL</i> channel counts	$0.37 \pm 0.11$	$0.26 \pm 0.07$	$0.43 \pm 0.12$	$0.46 \pm 0.23$
Ratio for the direct beam $= 0.93 \pm 0.03$				

<sup>11</sup> M. B. Stearns and B. D. McDaniel, Phys. Rev. **82**, 450 (1951).



TABLE IV. Values of  $E_{\max}$  obtained by comparing the experimental values for elastic scattering with the theoretical values derived under the assumption of a Rayleigh-type scattering of the gamma-rays. Two values of  $E_{\max}$  are obtained, the lower by assuming the scattered gamma-rays have energy greater than the resonant energy and the higher by assuming the incident gamma-rays have energy less than the resonant energy.  $x$  is the fraction of attraction exchange force for the  $n-p$  potential.

	$x=0$		$x=\frac{1}{2}$	
	Upper	Lower	Upper	Lower
Pb	$19.5^{+0.3}_{-0.2}$ Mev	$13.7^{+0.1}_{-0.3}$ Mev	$20.2^{+0.4}_{-0.3}$ Mev	$12.9^{+0.4}_{-0.5}$ Mev
Sn	$19.4^{+0.3}_{-0.2}$ Mev	$13.7 \pm 0.2$ Mev	$20.1^{+0.4}_{-0.2}$ Mev	$13.1^{+0.2}_{-0.5}$ Mev
Cu	$19.7^{+0.7}_{-0.4}$ Mev	$13.5^{+0.3}_{-0.8}$ Mev	$20.5^{+1.0}_{-0.5}$ Mev	$12.6^{+0.6}_{-1.0}$ Mev

scattered radiation with respect to the direct radiation, it is concluded that there must be a considerable amount of inelastic scattering present.

## VI. DISCUSSION OF RESULTS

Using gamma-rays with a 100-Mev bremsstrahlung spectrum, Gaertner and Yeater<sup>7</sup> obtained a cross section for Cu (assuming a 5-Mev total resonance width) of,  $(d\sigma/d\omega)_{116^\circ} < 0.4$  mb/sterad. The comparable measurement in this experiment yielded  $(d\sigma/d\omega)_{116^\circ} \geq 0.066 \pm 0.016$  mb/sterad, with an estimated upper limit of about 0.2 mb/sterad.

For the scattering of gamma-rays with a 22-Mev bremsstrahlung spectrum from Pb, Dressel *et al.*<sup>8</sup> obtained a value of  $(d\sigma/d\omega)_{116^\circ} \approx 1.5 \pm 0.7$  mb/sterad. This experiment yielded a value of  $(d\sigma/d\omega)_{116^\circ} \geq 1.2 \pm 0.2$  mb/sterad with an upper limit of about 3.6 mb/sterad.

The elastic nuclear scattering can be considered from the point of view of two limiting cases. In the first case we assume that the absorption curve is due to a single energy level of small width and also that the energy of the incident gamma-ray is many widths of the absorption curve away from the resonant energy, i.e., that the scattering takes place on the tail of the resonance curve, ordinary Rayleigh scattering. For the second case we assume that the absorption curve is widened; owing to, for example, many overlapping energy levels. We also assume that the energy of the incident gamma-ray is within a half-width of the peak of the absorption curve. (This is the case of resonance fluorescence.)

*Case 1.* Making the assumptions given above for the first case, the expression for the elastic nuclear scattering of gamma-rays can be easily obtained from the Kramers and Heisenberg dispersion formula.<sup>12</sup> The expression obtained is

$$\sigma_{Th} = \frac{8\pi}{3} r_0^2 \left( \frac{m}{M} \right)^2 \left( \frac{E^2}{E_{\max}^2 - E^2} \right)^2 \left( \frac{NZ}{A} (1 + 0.8x) \right)^2, \quad (5)$$

<sup>12</sup> W. Heitler, *Quantum Theory of Radiation* (Oxford University Press, London, 1944), second edition, p. 132.

where  $r_0$  is the classical radius of the electron,  $m$  is the mass of the electron,  $M$  is the mass of a nucleon,  $E$  is the energy of the gamma-ray,  $N$  is the number of neutrons in the scattering nucleus,  $Z$  is the number of protons in the scattering nucleus,  $A$  is the atomic number of the scattering nucleus,  $x$  is the fraction of attractive exchange force for the  $n-p$  potential, and  $E_{\max}$  is the energy at the maximum of the absorption excitation curve.

Since, if the value of  $x$  is assumed,  $E_{\max}$  is the only adjustable parameter in Eq. (5), we can determine values of  $E_{\max}$  by substituting the experimentally obtained elastic cross sections into this equation for  $\sigma_{Th}$ .

To obtain the total measured cross sections from the differential cross sections we must know the angular dependence of the cross sections. It is the same as the angular dependence for Thomson scattering, that is, a  $(1 + \cos^2\theta)$  dependence. Using this angular dependence, we get from the observed differential cross sections the following total elastic scattering cross sections:  $\sigma_{Pb} = 7.4 \pm 2.0$  mb,  $\sigma_{Sn} = 2.8 \pm 0.7$  mb, and  $\sigma_{Cu} = 0.62 \pm 0.28$  mb. Two values of  $x$  are assumed,  $x=0$  and  $x=\frac{1}{2}$ . For the value  $x=0$ , the  $n-p$  interactions are presumed to be due to only ordinary forces. While for the value  $x=\frac{1}{2}$ , the  $n-p$  interactions are assumed to be due to half exchange and half ordinary forces. The value of  $x=\frac{1}{2}$  for the attractive exchange force is in agreement with the Berkeley  $n-p$  scattering experiments.<sup>13</sup> For each element, two values of  $E_{\max}$  are obtained by substituting the observed cross sections into Eq. (5). These values of  $E_{\max}$  are given in Table IV.

From  $\gamma-n$ ,  $\gamma-\alpha$ , and  $\gamma-p$  excitation curves we know that most of the maxima fall between 15 and 21 Mev; therefore, the higher energy, nearer 20 Mev, is probably the value to be considered. However, having  $E_{\max} \sim 20$  Mev is in poor agreement with other evidence.<sup>14</sup> An integrated  $\gamma-n$  cross section of about 0.9 Mev-barns, with  $E_{\max} \sim 18$  Mev, has been observed for Cu.<sup>2,15</sup> The total integrated cross section predicted by Levinger and Bethe is  $\sigma_T = 0.94$  Mev-barns for  $x=0$  or 1.3 Mev-barns for  $x=\frac{1}{2}$ . Therefore, if  $E_{\max}$  were near 20 Mev, the gamma-ray absorption curve must continue increasing up to 20 Mev, and the total integrated cross section would become larger than the total oscillator strength permits. This then leads one to believe that the absorption of the gamma-rays may not be due purely to one single dipole level but may for some reason be due to a widened level. So let us now look at Case 2.

*Case 2.* In this case the assumption is made that the absorption curve is widened and that the incident gamma-ray energy is inside the width of the absorption

<sup>13</sup> Hadley, Kelly, Leith, Segrè, Wiegand, and York, Phys. Rev. 75, 351 (1949).

<sup>14</sup> P. Morrison (private communication).

<sup>15</sup> Johns, Katz, Douglas, and Haslam, Phys. Rev. 80, 1062 (1950); Katz, Johns, Baker, Haslam, and Douglas, Phys. Rev. 82, 271 (1951).

curve. In this case Eq. (5) becomes<sup>16</sup>

$$\sigma_{Th} = \frac{2\pi}{3} r_0^2 \left( \frac{m}{M} \right)^2 \left[ \frac{NZ}{A} (1 + 0.8x) \right]^2 \frac{E^2}{(E_{max} - E)^2 + (\delta/2)^2},$$

where  $\delta$  is the full width of the absorption curve.

For this case let us assume that  $E_{max}$  is around 17–18 Mev; then  $\delta$  is the only adjustable parameter. Substituting the experimental cross section into Eq. (6) for  $\sigma_{Th}$  we get a width of  $\delta \sim 4$  Mev for  $x=0$  and a width of  $\delta \sim 5.5$  Mev for  $x=\frac{1}{2}$ . The observed widths from  $\gamma-n$  excitation curves are about 5 Mev. Therefore, it is seen that by using values of  $E_{max}$  around 17–18 Mev with the assumption of a broad resonance, this model gives good agreement with the observed  $\gamma-n$  widths.

The data from this experiment, whether treated under Case 1 or Case 2, give no evidence that  $E_{max}$  has any dependence on  $Z$ .

The models used in the above two cases are the limiting cases of wide and narrow resonances. From the elastic scattering results alone, we are unable to distinguish between the two cases. However, the  $\gamma-n$  results and the  $\gamma-\gamma$  results obtained here would tend to favor a wide level theory with the maximum of the absorption curve around 17–18 Mev and a full width of from 4 to 6 Mev. Both of the models assumed above are one-level theories, and while they give qualitative agreement with the observed elastic scattering they are not very trustworthy quantitatively.

The large amount of inelastic scattering observed indicates that the Goldhaber-Teller model, of the nucleus vibrating as a whole in only one main mode, cannot be correct without modification. This is as expected, since this model is intentionally extreme and assumed primarily because it is easy to handle in calculations.

To interpret the high  $Z$  dependence of the inelastic scattering ( $> Z^{2.9}$ ), let us consider the inelastic scattering process in two steps. In the first step the gamma-ray is absorbed by a group of nucleons in the nucleus. (This absorption process is roughly proportional to  $Z$ .) The energy of the gamma-ray then becomes shared among all the nucleons, forming a compound state of the nucleus. The second step is then the de-excitation of the compound nucleus. One would expect the decay of the compound nucleus to depend quite strongly on the

number of nucleons in the nucleus. We can get a rough idea of this dependence if we know the energy level density at the various energies and the probability of the nucleus to emit a given energy gamma-ray. By multiplying these two quantities together and integrating over the energy region corresponding to the detected gamma-rays, we can obtain an estimate of the  $Z$  dependence for the emission of gamma-rays.

If one uses Weisskopf's expression for the energy level density,<sup>17</sup>  $\omega \simeq C \exp[1.6(A-40)^{1/2}E]^{1/2}$ , and assuming mainly dipole transitions, where the probability of emission of gamma-rays goes as  $(E_\gamma)^3$ ,  $(E_\gamma = 17.6 - E)$ , one obtains

$$\sigma_{inel} \sim \int_{E=0}^{E=5.3 \text{ Mev}} (17.6 - E)^3 \exp[1.6(A-40)^{1/2}E]^{1/2} dE. \quad (7)$$

An upper limit of 5.3 Mev is used, since the *HL* channel detected gamma-rays greater than 12.3 Mev. If one evaluates this quantity, it is, of course, not a function of a single power of  $Z$ , but for the elements Cu, Sn, and Pb it varies roughly as  $Z^4$ . This then shows that considering the inelastic scattering as a dipole absorption of the gamma-rays followed by the formation and subsequent decay of a compound state of the nucleus leads to the inelastic scattering cross section being a strongly dependent function of  $Z$  ( $\sim Z^5$  for this model). The above estimate of the variation with  $Z$  is very crude, since the statistical model is applied to energy levels in the region between 0 and 5.3 Mev where this model is not very suitable. Also it has been assumed that the gamma-ray transitions from the compound nucleus are due to only dipole transitions, which is probably not true for these high energy gamma-rays.

It is seen that the general results of the experiment can be qualitatively understood by using very simplified models of the nucleus. However, much more realistic and detailed calculations must be made, assuming various models for the subunits in the nucleus, before the experimental results are understood quantitatively.

It is a pleasure to thank Professors B. D. McDaniel and P. Morrison for their helpful discussions and suggestions throughout the course of this work. I also wish to thank Professor Bethe for several valuable discussions, and I am grateful to Dr. Robert S. Rochlin for the use of his tritium target.

<sup>16</sup> See, for example, reference 13, p. 38.

<sup>17</sup> See reference 2, p. 412.